

Supplementary Information for

**Structure and Compositional Control of MoO<sub>3</sub> Hybrids  
Assembled by Nanoribbons for Improved Pseudocapacitor  
Rate and Cycle Performance**

**Qasim Mahmood, Woo Sik Kim\* and Ho Seok Park\***

*Department of Chemical Engineering, College of Engineering, Kyung Hee University,  
Yongin-si 446-701, Republic of Korea, E-mail: phs0727@khu.ac.kr*

## Experimental Section:

**Chemicals.** HMimCl IL, MoCl<sub>5</sub> precursor, ethanol, and Nafion (perfluorinated resin solution, 5 wt% in lower aliphatic alcohol and water mixture) were purchased from Aldrich.

**Synthesis of hierarchically structured MoO<sub>3</sub> with Hybrid composition.** H-MoO<sub>3</sub> NHs was synthesized by sol-gel method. MoCl<sub>5</sub> was used as precursor material. In a typical synthesis of H-MoO<sub>3</sub> NHs, 0.14823 g of HMimCl was added to 2 ml of ethanol and then 0.4 g of MoCl<sub>5</sub> precursor was poured followed by 2 h stirring. It resulted in homogeneous brown-greenish solution, which was heated to 200 °C for 18 hours. After an ionothermal process, H-MoO<sub>3</sub> NHs were obtained. The resulting materials were washed with the deionized water at several times and then dried in oven before characterization and electrochemical application. H-MoO<sub>3</sub> control sample was synthesized in the same manner to H-MoO<sub>3</sub> NHs and then ILs were completely removed from hybrids by using the soxhlet apparatus with acetonitrile as solvent. C-MoO<sub>3</sub> was synthesized as the other control sample and all synthesis processes performed without ILs were the same as those of hybrid sample.

**Electrochemical measurements.** CV measurements were carried out using a three electrode system. Glassy carbon electrode was used as a working electrode, Ag/AgCl as reference electrode, and Pt wire as a counter electrode. 1 M of aqueous H<sub>2</sub>SO<sub>4</sub> solution was used as an electrolyte. Glassy carbon electrode was coated by H-MoO<sub>3</sub> NHs as follows. 10 mg of H-MoO<sub>3</sub> NHs were sonicated in 5 ml of Nafion solution until a uniform and homogeneous ink was achieved. 5 μl of this suspension was dropped onto glassy carbon electrode which was polished before the measurement. This electrode was dried in a vacuum oven at 80 °C for 20 min to remove the solvent and then used as working electrode. All potentials were referred to Ag/AgCl reference electrode. Galvaostatic charge/discharge curves were measured at a specific current from 1.3 A g<sup>-1</sup> to 27.0 A g<sup>-1</sup> using two electrode system.

**Characterization.** TEM images were collected on a JEM-3010 high-resolution transmission electron microscope (HR TEM, 300 kV). FT-IR spectra were collected on a JASCO FT-IR 470 plus. Each spectrum was recorded from 4000 to 500 cm<sup>-1</sup> with using 12 scans at a resolution of 4 cm<sup>-1</sup>. XRD data were obtained on a Rigaku D/max III C (3 kW) with a  $\theta/\theta$  goniometer equipped with a CuK $\alpha$  radiation generator. The diffraction angle of the diffractograms was in the range of  $2\theta = 2-50^\circ$ . XPS data were obtained using a Thermo MultiLab 2000 system. Al Mg $\alpha$  X-ray source at 200 W was used with pass energy of 20 eV and 45° takeoff angle under 10<sup>-7</sup> Torr vacuum

analysis chamber. After a background correction, curve fitting was carried out using a mixed Gaussian-Lorentzian function. To compensate for charging effects, binding energies were corrected after curve fitting. TGA were carried out using a Dupont 2200 thermal analysis station. TGA data was collected at a heating rate of  $10\text{ }^{\circ}\text{C min}^{-1}$  in air. The electrochemical characteristics of SC devices were evaluated by CV curves using a CHI 760D electrochemical workstation (CH Instruments) at room temperature. In addition, galvaostatic charge/discharge and impedance spectroscopy measurements were performed using a Solartron 1260.

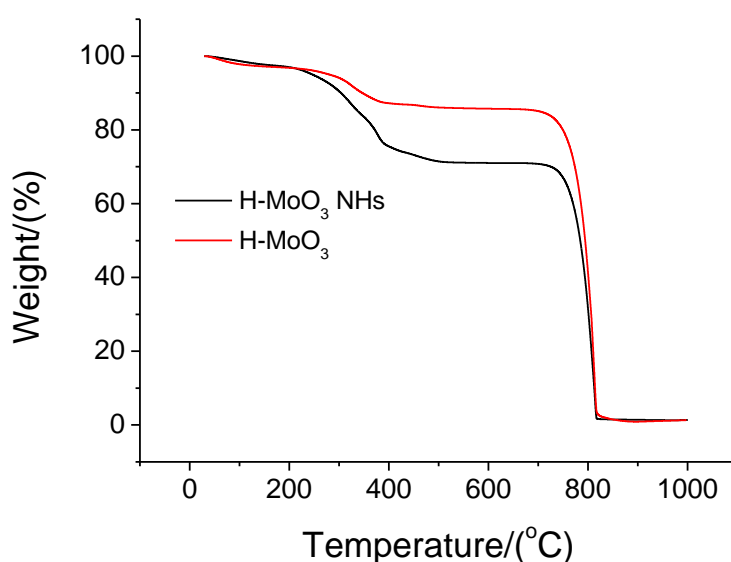


**Fig. S1** TGA curves of H-MoO<sub>3</sub> and H-MoO<sub>3</sub> NHs.

To quantitatively analyze hybrid sample (H-MoO<sub>3</sub> NHs), a control sample (H-MoO<sub>3</sub>) was synthesized following the same way as hybrid sample and thus ILs were removed carefully with acetonitrile solvent using soxhlet apparatus. The composition of hybrid was estimated by TGA analysis of both samples. As shown in Figure S1, two samples had almost the same weight loss of ~ 15 wt% up to 350 °C, which was attributed to the removal of physically and chemically adsorbed water. H-MoO<sub>3</sub> NHs showed the weight loss of ~ 13 wt% in the range of 350 - 500 °C due to the thermal decomposition of ILs, while H-MoO<sub>3</sub> revealed only ~ 2 wt%. These results indicate that ~ 98 % of ILs were removed from the hybrid sample using soxhlet apparatus with acetonitrile. Moreover, two samples exhibited further weight loss above 500 °C because of the sublimation of MoO<sub>3</sub>.<sup>[1-3]</sup>



**Fig. S2** Photo image of the dispersion of C-MoO<sub>3</sub> in acetonitrile and H-MoO<sub>3</sub> NHs in acetonitrile, dimethyl formamide, and water (from left to right).

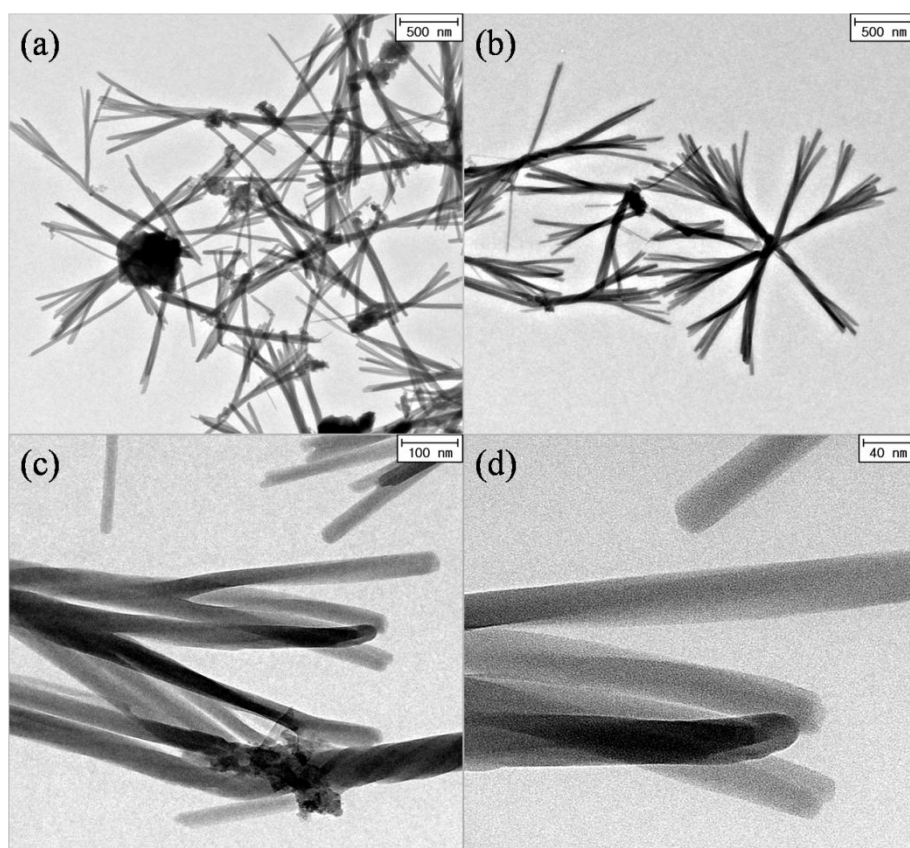


**Fig. S3** TEM images of H-MoO<sub>3</sub> NHs at different places and magnification scales.

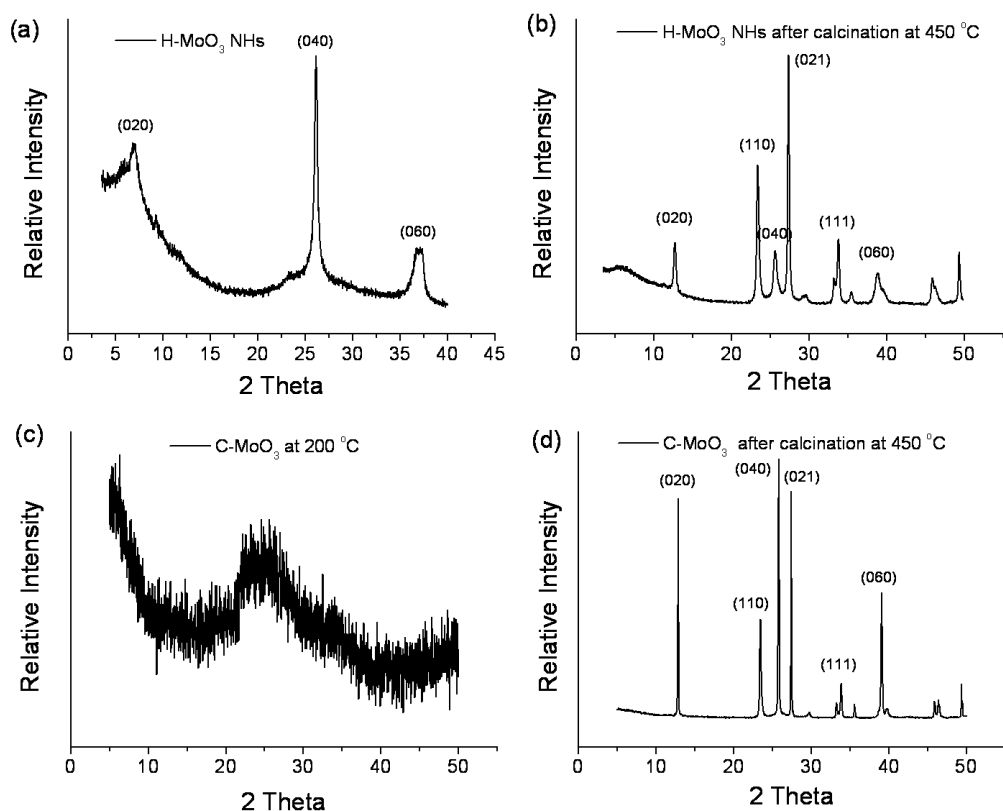


**Fig. S4** (a) and (b) XRD spectra of H-MoO<sub>3</sub> NHs before, and after calcination at 450 °C, (c) and (d) XRD spectra of C-MoO<sub>3</sub> before, and after calcination at 450 °C.

As shown in Fig. S4, the orthorhombic  $\alpha$ -MoO<sub>3</sub> phase remained intact with the emergence of (110), (021), and (111) peaks after calcination of H-MoO<sub>3</sub> NHs. ILs were completely removed after calcination at 450 °C, which exceeds the decomposition temperature of  $\sim$  350 °C. In particular, (020) peak of  $\alpha$ -MoO<sub>3</sub> in hybrids was shifted from  $2\theta=7.3$  to  $2\theta=12.8$  after completely removing ILs by calcination. This finding indicates the enlarged interlayer distance of MoO<sub>3</sub> by the IL coating.

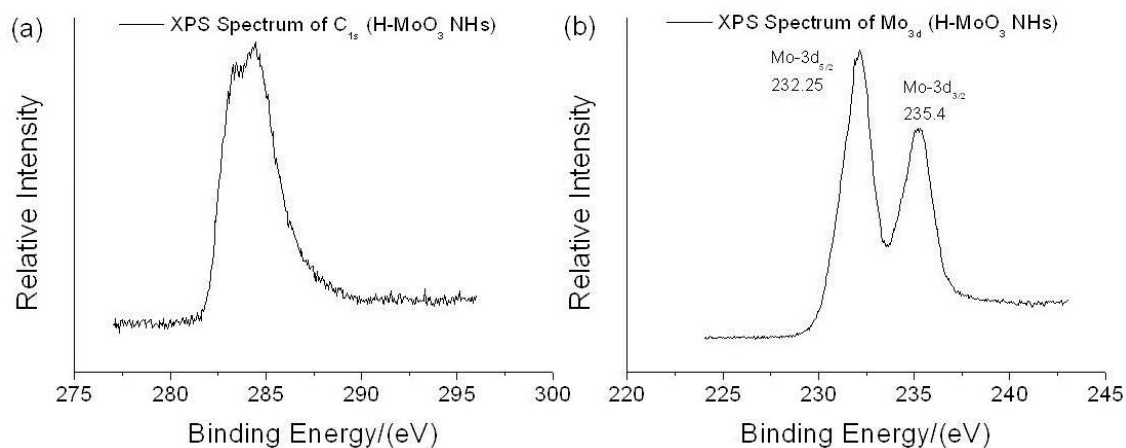


**Fig. S5** High resolution XPS scans of (a) C<sub>1s</sub> and (b) Mo<sub>3d</sub> of H-MoO<sub>3</sub> NHs.

XPS data of H-MoO<sub>3</sub> NHs further confirmed the formation of  $\alpha$ -MoO<sub>3</sub> with an oxidation state of Mo<sup>6+</sup> and nearly perfect Mo/O ratio of 1/3 as shown in Fig. S5. The presence of ILs in the hybrid was observed by the intense C<sub>1s</sub> peak. Mo<sub>3d</sub> peak showed the presence of two well-resolved spectral lines at 232.3 eV and 235.4 eV corresponding to the Mo<sub>3d5/2</sub> and Mo<sub>3d3/2</sub> spin orbit components of  $\alpha$ -MoO<sub>3</sub>, respectively. Furthermore, Mo<sub>3p3/2</sub> and O<sub>1s</sub> peaks of  $\alpha$ -MoO<sub>3</sub> were detected at 398.0 eV and 531.1 eV, respectively. These XPS results confirmed the hybrid composition of H-MoO<sub>3</sub> NHs and  $\alpha$ -phase of MoO<sub>3</sub>.<sup>[4]</sup>

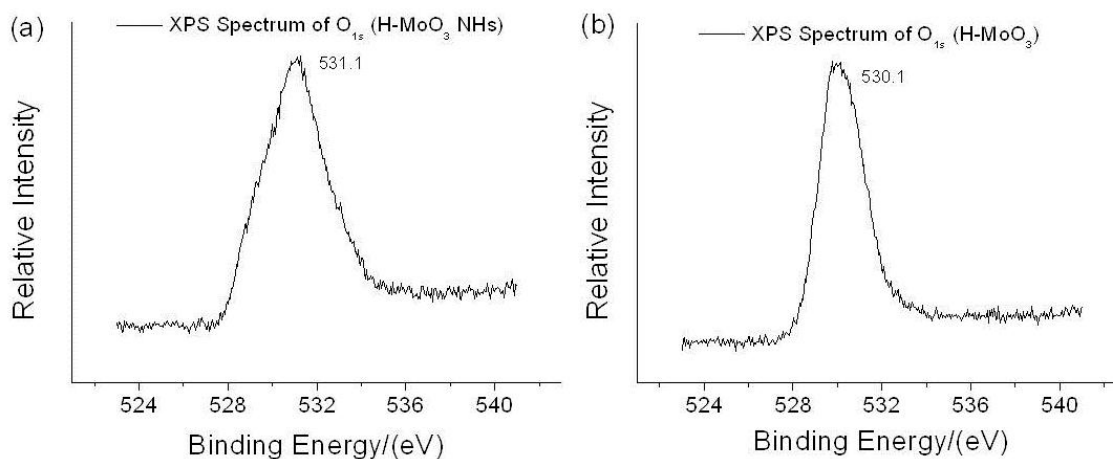


**Fig. S6** High resolution XPS scans of O<sub>1s</sub> of (a) H-MoO<sub>3</sub> NHs and (b) H-MoO<sub>3</sub>.

To verify the interactions between ILs and MoO<sub>3</sub>, O<sub>1s</sub> peaks of H-MoO<sub>3</sub> NHs and H-MoO<sub>3</sub> were compared in XPS survey spectra. O<sub>1s</sub> peak of H-MoO<sub>3</sub> NHs was shifted from 531.1 eV to 530.1 eV after removing IL by soxhlet extraction. O<sub>1s</sub> peak of H-MoO<sub>3</sub> NHs became broadened due to the different chemical circumstances attributable to the complex interactions of ILs with MoO<sub>3</sub> through hydrogen bonding-co- $\pi$ - $\pi$  stacking as shown in FT-IR spectra.



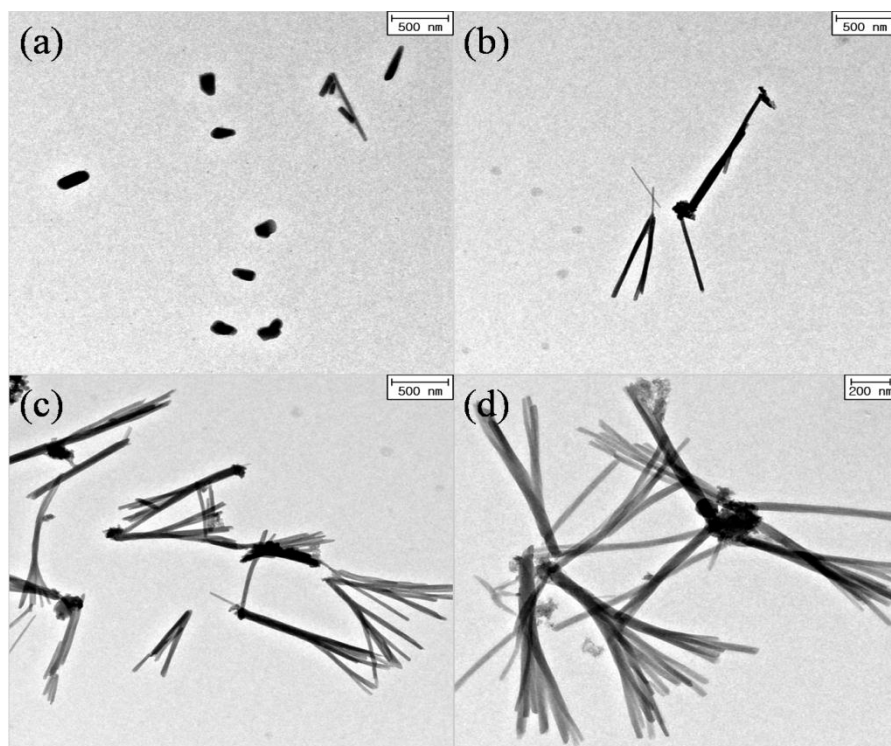


**Fig. S7** TEM images of H-MoO<sub>3</sub> NHs during an ionothermal treatment of (a) 1 hour, (b) 3 hours, (c) 5 hours, and (d) 7 hours at 200 °C.

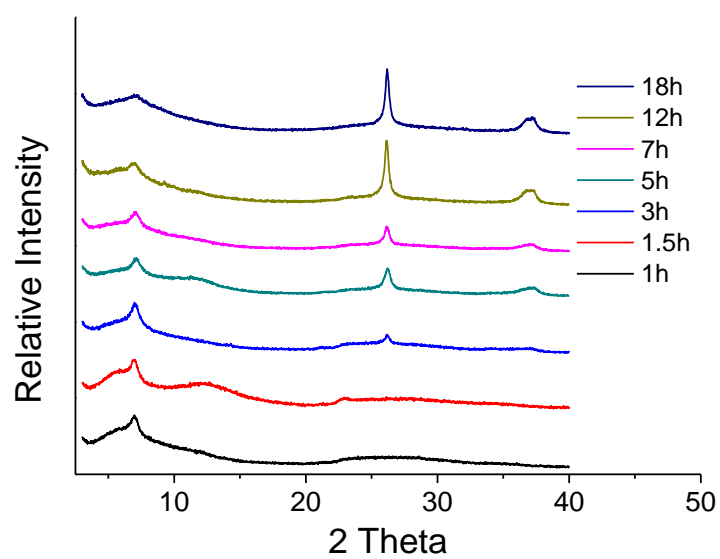


**Fig. S8** Reaction time-dependent XRD spectra of H-MoO<sub>3</sub> NHs during an ionothermal treatment at 200 °C.

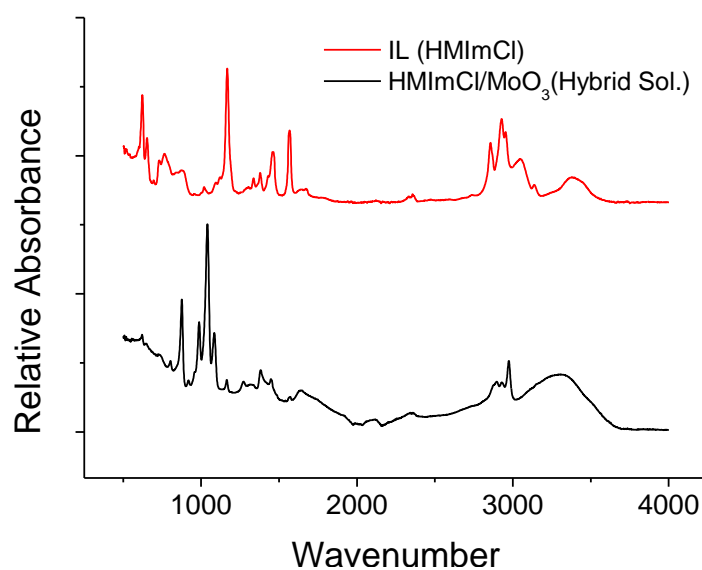


**Fig. S9** FT-IR spectra of pure HMIImCl IL and HMIImCl/MoO<sub>3</sub> hybrid solution.

To observe the interactions between ILs and  $\alpha$ -MoO<sub>3</sub>, FT-IR spectra of pure ILs and hybrids were analyzed. In the case of pure ILs, the peaks at 1500-1600 cm<sup>-1</sup> are assigned to vibration of aromatic C=N and C=C, while the peaks at 1100 cm<sup>-1</sup> are ascribed to vibration of C-N. The peaks at 2800-2900 cm<sup>-1</sup> and 3000-3200 cm<sup>-1</sup> are assigned to C-H stretching vibrations of alkyl chain and imidazolium ring, respectively. As shown in the spectra of hybrid, the peaks below 1000 cm<sup>-1</sup> are attributed to MoO<sub>3</sub>. The peak at 988 cm<sup>-1</sup> is associated with Mo=O stretching vibration, which is an indication for the layered orthorhombic MoO<sub>3</sub> phase.<sup>[5,6]</sup> The peak at 875 cm<sup>-1</sup> is assigned to the stretching vibrations of O atoms in Mo-O-Mo units of MoO<sub>3</sub>.<sup>[5,6]</sup> In particular, the peak of ILs at 1100 cm<sup>-1</sup> attributable to C-N stretching vibration mode of the imidazolium ring is very crucial for examining the  $\pi$ - $\pi$  stack of imidazolium rings.<sup>[7]</sup> It is concluded that the peak shifts of imidazolium ring and anion in hybrid toward the lower wavenumbers was attributed to hydrogen bonding-co- $\pi$ - $\pi$  stacking interactions.

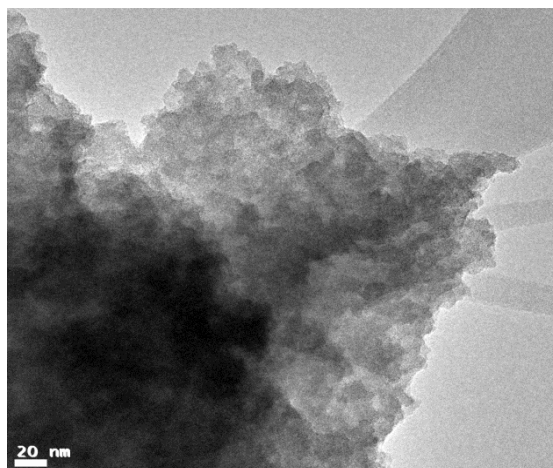


**Fig. S10** TEM image of C-MoO<sub>3</sub> synthesized by conventional sol-gel method.

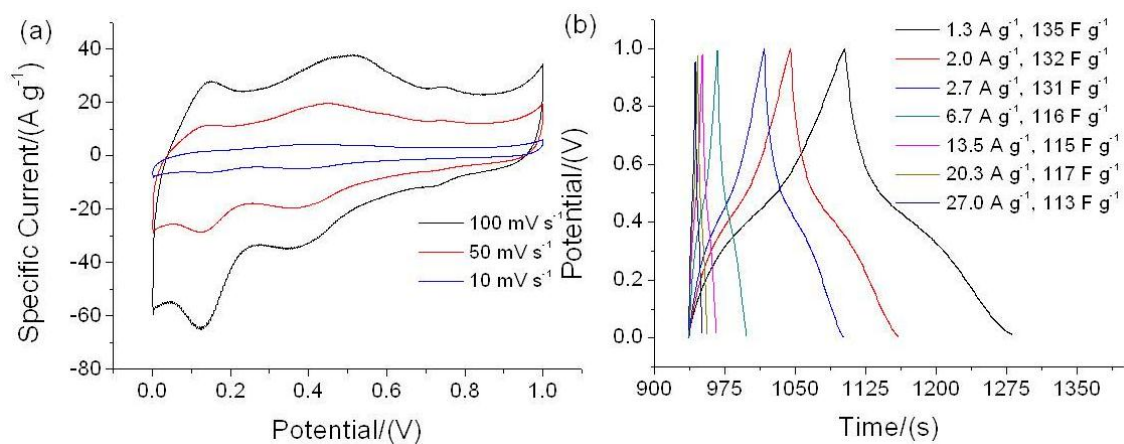


**Fig. S11** (a) CV curves of H-MoO<sub>3</sub> NHs as a function of scan rate (1.3 V s<sup>-1</sup> to 27.0 V s<sup>-1</sup>) and (b) galvanostatic charge/discharge curves of H-MoO<sub>3</sub> NHs as a function of specific current (1.3 A g<sup>-1</sup> to 27.0 A g<sup>-1</sup>).

## Supplementary References

- [1] R. F. de Farias, M. S. Refat, H. A. Hashem, *J. Incl. Phenom. Macrocycl. Chem.* **2008**, *61*, 113.
- [2] J. M. Vivar, T. Lopez, A. Campero, *Langmuir* **1991**, *7*, 704.
- [3] W. Dong, B. Dunn, *J. Mater. Chem.* **1998**, *8*, 665.
- [4] J. G. Choi, L. T. Thompson, *Applied Surface Science* **1996**, *93*, 143.
- [5] W. Dong, A. N. Mansour, B. Dunn, *Solid State Ionics* **2001**, *144*, 31.
- [6] L. Cheng, M. Shao, X. Wang, H. Hu, *Chem. Eur. J.* **2009**, *15*, 2310.
- [7] Y. Zhou, J. H. Schattka, M. Antonietti, *Nano Lett.* **2004**, *4*, 477.